

Stepwise “Click” Chemistry for the Template Independent Construction of a Broad Variety of Cross-Linked Oligonucleotides: Influence of Linker Length, Position, and Linking Number on DNA Duplex Stability

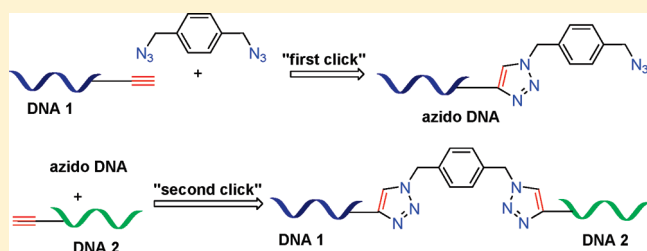
Hai Xiong^{†,‡} and Frank Seela^{*,†,‡}

[†]Laboratory of Bioorganic Chemistry and Chemical Biology, Center for Nanotechnology, Heisenbergstrasse 11, 48149 Münster, Germany

[‡]Laboratorium für Organische und Bioorganische Chemie, Institut für Chemie, Universität Osnabrück, Barbarastrasse 7, 49069 Osnabrück, Germany

Supporting Information

ABSTRACT: Cross-linked DNA was constructed by a “stepwise click” reaction using a bis-azide. The reaction is performed in the absence of a template, and a monofunctionalized oligonucleotide bearing an azido-function is formed as intermediate. For this, an excess of the bis-azide has to be used compared to the alkynylated oligonucleotide. The cross-linking can be carried out with any alkynylated DNA having a terminal triple bond at any position of the oligonucleotide, independent of chain length or sequence with identical or nonidentical chains. Short and long linkers with terminal triple bonds were introduced in the 7-position of 8-aza-7-deaza-2'-deoxyguanosine (1 or 2), and the outcome of the “stepwise” click and the “bis-click” reaction was compared. The cross-linked DNAs form cross-linked duplexes when hybridized with single-stranded complementary oligonucleotides. The stability of these cross-linked duplexes is as high as respective individual duplexes when they were ligated at terminal positions with linkers of sufficient length. The stability decreases when the linkers are incorporated at central positions. The highest duplex stability was reached when two complementary cross-linked oligonucleotides were hybridized.



INTRODUCTION

DNA interstrand cross-links (ICLs) are mutagenic if not repaired.¹ Cross-linking is specific to particular DNA nucleobases.^{2,3} Cross-links shut down gene replication,¹ and cross-linking drugs are used in cancer chemotherapy.⁴

Bifunctional reagents such as nitrogen mustards, nitrosoureas, or platinum compounds can covalently connect nucleobases, which ultimately leads to the interstrand cross-linking.^{1,4} Alternatively, interstrand cross-links can be induced by light⁵ or γ irradiations⁶ as well as with naturally occurring molecules such as mitomycin,⁷ psoralen,⁸ etc.

The copper catalyzed azide–alkyne Huisgen–Meldal–Sharpless cycloaddition “click” reaction (CuAAC)^{9–11} has been applied to nucleoside and oligonucleotide functionalization^{12–18} and to cross-linking.^{19–23} The bio-orthogonal nature has increased the credentials of this reaction which is suitable to be performed in vitro and even in vivo.^{24–26} The created 1,2,3-triazole system is inert to functional groups present in nucleic acids, proteins, and other cellular components and is stable at physiological pH. Our laboratory has reported on the “click” functionalization of the four DNA building blocks modified with diynyl side chains at the 5-position of pyrimidine bases and the 7-position of 7-deazapurine or 8-aza-7-deazapurine residues.²⁷

As bis-azides are easily accessible,^{28–30} we have used them to cross-link DNA in one step in a template independent way with alkynyl linkers.²³ By the so-called “bis-click” protocol, only identical strands can be cross-linked in a selective way; non-identical strands lead to more than one cross-linked species.²³ Four-stranded DNA consisting of two cross-linked oligonucleotide duplexes was obtained after hybridization.

Continuing our research on cross-linking of DNA led to the development of the “stepwise click” strategy. This approach offers the possibility to cross-link nonidentical oligonucleotides with short or long linker arms selectively at identical or different linking positions. For this, a large excess of a bis-azide is used leading to a monofunctionalized azide (“first click”). This azide intermediate is isolated, and then a “second click” is performed with an alkynylated oligonucleotide leading to the cross-linked product. This “stepwise click” reaction was now carried out on nucleosides and oligonucleotides. 8-Aza-7-deaza-2'-deoxyguanosine with short (1) and long linker (2) arms was employed in the “stepwise click” protocol together with the cross-linking reagent

Received: March 7, 2011

Published: May 18, 2011

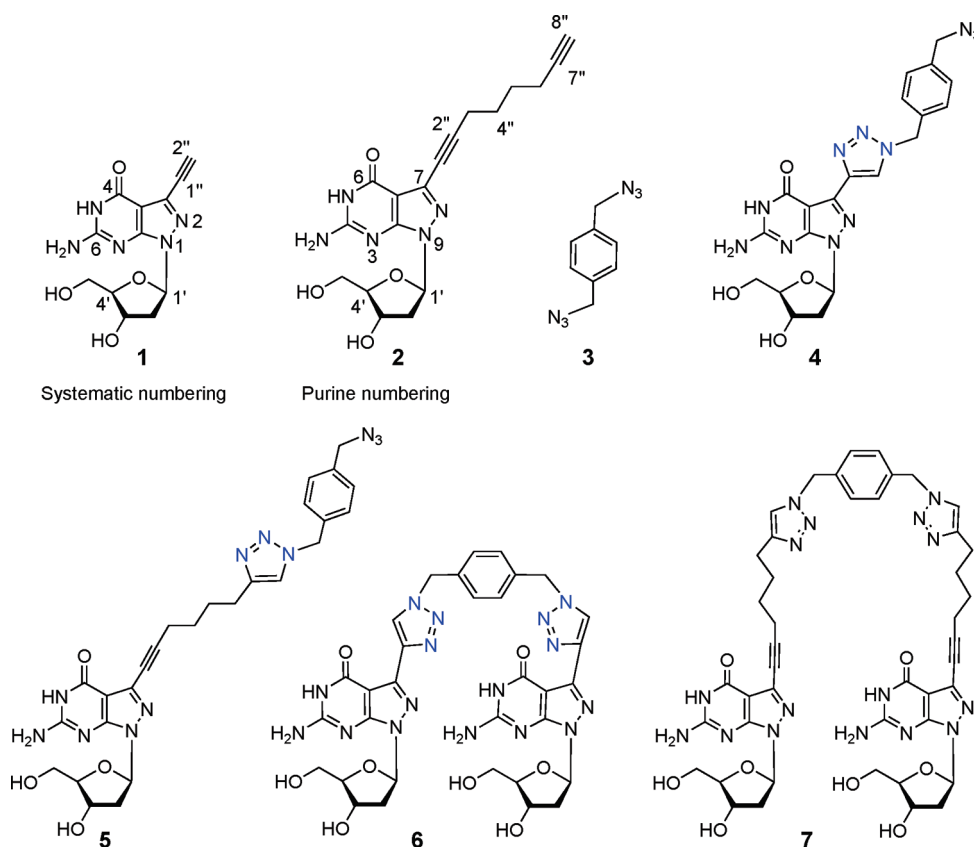


Figure 1. Structures of nucleosides and mono- and bis-functionalized adducts used in this study.

azido-*p*-xylene **3**. The first click reaction afforded the monofunctionalized azido intermediates **4** and **5**, while the cross-linked nucleosides **6** and **7** were formed in the second click reaction (Figure 1).

The ethynylated and octadiynylated 8-aza-7-deaza-2'-deoxyguanosines **1** and **2** were incorporated into a series of 12-mer oligonucleotides. These oligonucleotides bearing diynyl side chains with terminal triple bonds at various positions were ligated using azido-*p*-xylene (**3**) as cross-linking reagent. Thus, by employing the “stepwise click” protocol, any DNA oligonucleotide can be cross-linked selectively.

Novel cross-linked four-stranded duplexes were constructed from cross-linked single strands. For this, hybridization experiments were performed. Complementary free single-stranded oligonucleotides as well as cross-linked strands were hybridized with the cross-linked oligonucleotides. The novel DNA constructs were evaluated with respect to the influence of linker length, linking position and number of the modification sites.

RESULTS AND DISCUSSION

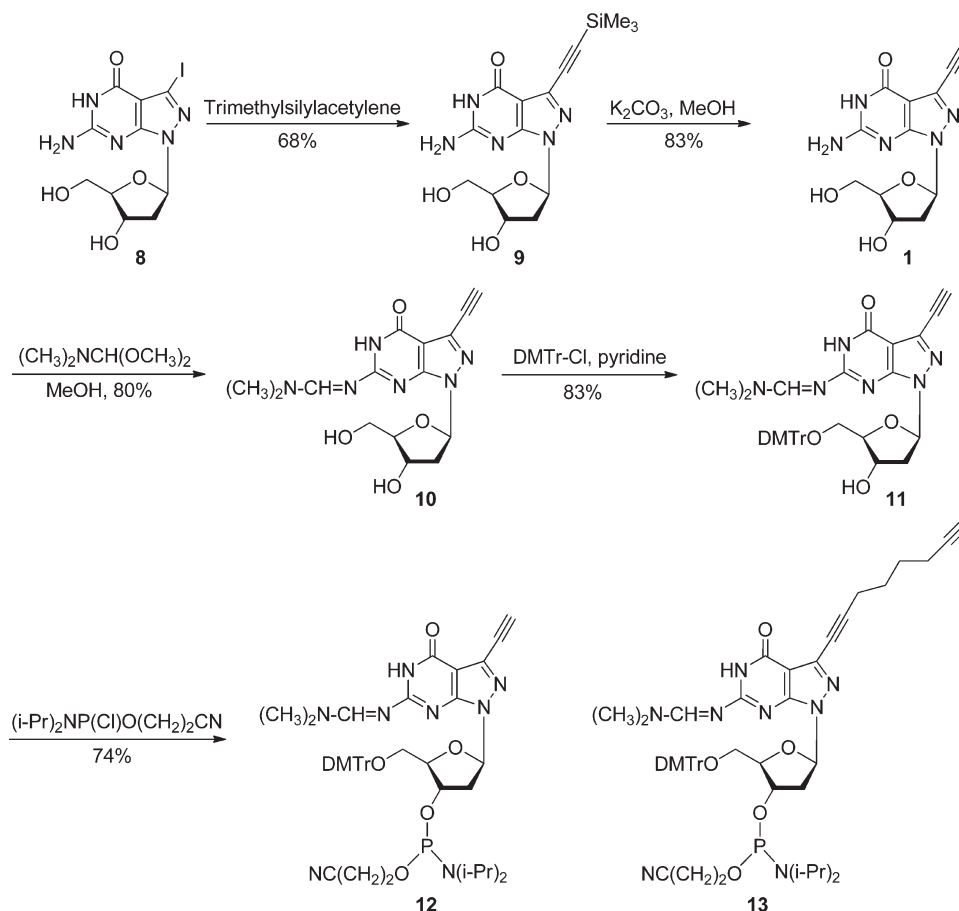
1. Synthesis and Characterization of Monomers. 7-Iodo-8-aza-7-deaza-2'-deoxyguanosine (**8**)³¹ was used as starting material for the synthesis of the phosphoramidite **12**. Nucleoside **1** was synthesized by Sonogashira cross-coupling. The reaction was performed in dry DMF in the presence of Et₃N, [Pd⁰(PPh₃)₄], and CuI, with a 7-fold excess of trimethylsilyl acetylene affording **9** (68%). The trimethylsilyl derivative was deprotected using K₂CO₃ in methanol affording compound **1** (83%). Nucleoside **1** was protected with the *N,N*-dimethylaminomethylidene residue to give the derivative **10** (80% yield). 4,4'-Dimethoxytritylation

under standard conditions furnished the 5'-*O*-DMT derivative **11** (83% yield). Phosphitylation with 2-cyanoethyl *N,N*-diisopropylphosphoramidochloridite furnished the phosphoramidite **12** (74%) (Scheme 1). The synthesis of the phosphoramidite **13** has already been reported.^{27c}

Next, the potential of the bis-azide **3** in the cross-link reaction was studied on nucleosides. For this, the click reaction was performed at room temperature on nucleosides **1** or **2** with the bis-azide **3** in a mixture of THF/H₂O/*t*-BuOH with CuSO₄ · 5 H₂O as catalyst and sodium ascorbate as reducing agent. The starting material was consumed within 12 h. Under these conditions, monofunctionalization occurred when the molar excess of the bis-azide **3** over the nucleosides **1** or **2** was 5: 1, while bis-adducts were formed when the bis-azide/nucleoside ratio was 0.5:1 (Scheme 2). In the bis-click reaction with **1**, the cross-linked product **6** precipitated. Because of its low solubility it could not be chromatographed but was pure (52% yield) after the filter cake was washed with methanol and water. From the washing solution, the monofunctionalized intermediate **4** was isolated in 7% yield (Experimental Section). The corresponding reaction with compound **2**, which is shown in the second part of the Scheme 2, has already been reported.²³

All compounds were characterized by elemental analyses as well as by their ¹H and ¹³C NMR spectra. The ¹³C NMR chemical shifts are listed in the Experimental Section (see Table 6). NMR chemical shift signals were assigned by ¹H–¹³C gated-decoupled spectra as well as by DEPT-135 NMR spectra (Table S1, Supporting Information). The monofunctionalized adduct **4** and the bis-click adduct **6** can be easily identified by ¹H NMR spectroscopy. For compound **4**, the two

Scheme 1. Synthesis of Phosphoramidite 12



methylene bridges of the 1,4-phenylene moiety show two separate singlets (5.75 ppm and 4.45 ppm; Figure S46, Supporting Information), while only one singlet is presented in compound **6** (5.72 ppm; Figure S54, Supporting Information). Further confirmation for mono- vs bifunctionalized compounds was obtained from the intensity ratio of the H-triazole (8.95 ppm) vs 1,4-phenylene-H signals (7.33–7.41 ppm) (Figure S46, Supporting Information). The ratio is 1:4 for the monofunctionalized compound **4** containing one triazole ring (1H, H-triazole) and one 1,4-phenylene residue (4H, H-arom). The bis-click compound **6** containing two triazole rings (2H, 2 × H-triazole) and one 1,4-phenylene ring (4H, H-arom) shows an intensity ratio (H-triazole vs 1,4-phenylene-H) of 2:4 (Figure S54, Supporting Information). In the same way, it can be distinguished between the monofunctionalized compound **5** and the bis-click adduct **7**.

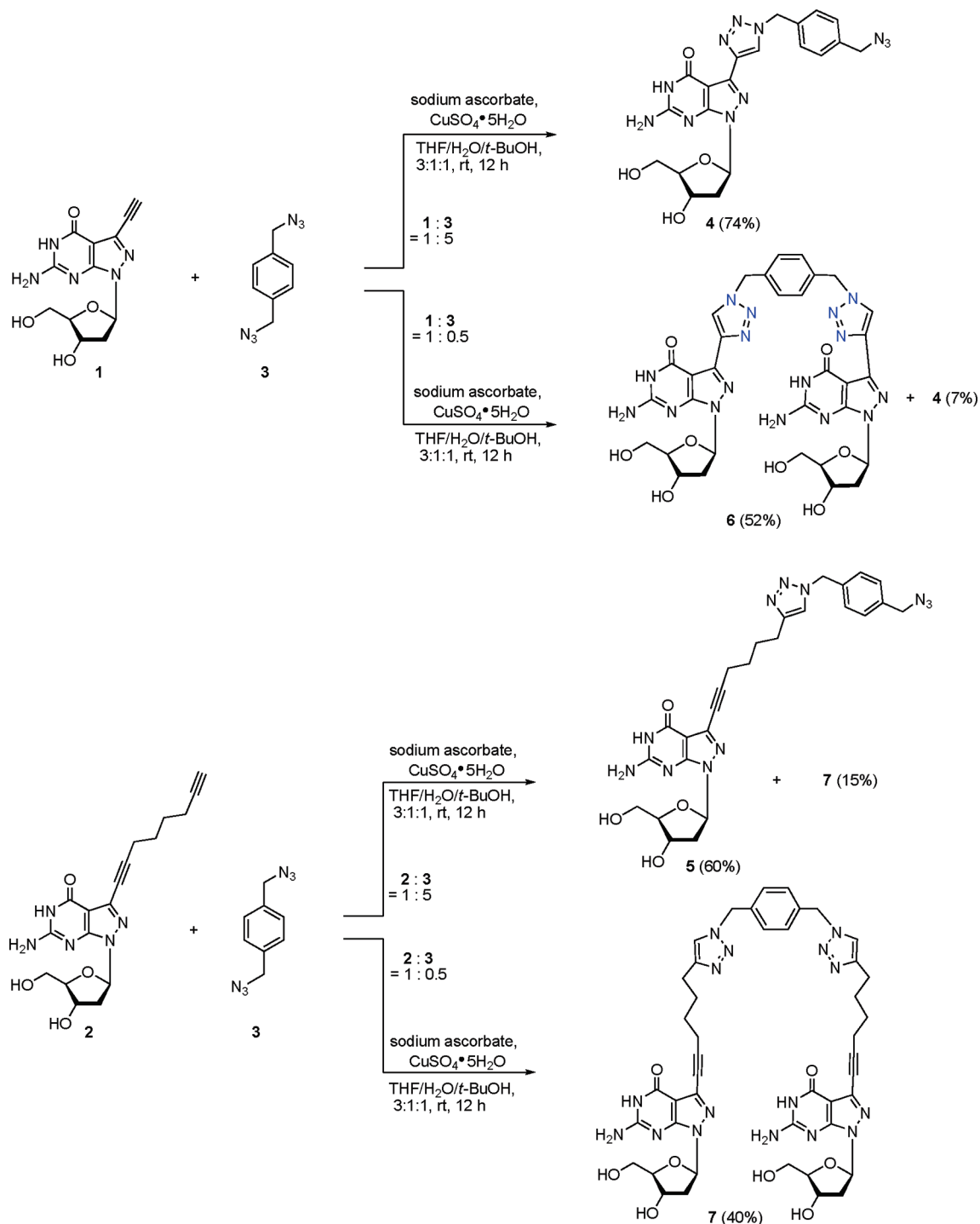
2. Evaluation of the Effect of Linker Lengths and Position of Nucleosides 1 or 2 on Oligonucleotide Duplexes. In order to evaluate the influence of side chains (long and short linker arms and different linking positions) on the DNA duplex stability, a series of oligonucleotides were prepared by solid-phase synthesis using the phosphoramidite **12** or **13** as well as standard phosphoramidites. The syntheses were performed at 1 μ mol scale. The coupling yields were always higher than 95%. Deprotection of the oligomers was performed in aqueous NH_3 (25%) at 60 $^\circ\text{C}$ for 14 h. The oligonucleotides were purified before and after detritylation by reversed-phase HPLC. The

homogeneity of the oligonucleotides was confirmed by HPLC analysis, and their molecular weights were determined by LC-ESI-TOF or MALDI-TOF mass spectrometry (Table S2, Supporting Information).

Single replacements of dG by compound **1** at various positions of the reference duplex 5'-d(TAG GTC AAT ACT) (ODN-**14**) and 3'-d(ATC CAG TTA TGA) (ODN-**15**) were performed, and the duplex stability was investigated by T_m measurements. The T_m values listed in Table 1 were determined at high salt (1 M NaCl) conditions at pH 7.0 with a 5 μM concentration of the single strands. T_m values at low salt (0.1 M NaCl) are generally 3 $^\circ$ lower.^{27c} From Table 1 the following conclusions can be drawn: (i) replacement of one dG residue by nucleoside **1** (duplexes **14**·**16**, **14**·**17**, and **18**·**15**) increases the T_m value ($\Delta T_m = +2.5$ –3 $^\circ\text{C}$) compared to the reference duplex **14**·**15**. (ii) The T_m changes found for oligonucleotide duplexes containing 8-aza-7-deaza-7-ethynyl-2'-deoxyguanosine (**1**) are similar to those incorporating the octadiynyl compound **2**. (iii) The less space demanding ethynyl side chain has almost the same positive influence on DNA duplex stability as the long octadiynyl linker. The positioning of the modified nucleoside is of less importance. The melting hypochromicity (% h) of the oligonucleotide duplexes is in the range of 15–17%.

3. Comments to the "Click" Cross-Linking of Alkynyl Oligonucleotides with Bis-azides. Azido groups as well as terminal triple bonds display functionalities which are highly exergonic during adduct formation. Both functionalities were

Scheme 2. Synthesis of the Monofunctionalized Conjugates 4 and 5 and the Bis-adducts 6 and 7



already introduced previously in individual oligonucleotide strands, and “click” reactions thereof were performed by copper(I) salt assistance.^{15–17,20,21,23}

The presence of the azido group and the triple bonds in two separate strands leads to only one “clicked” cross-linked product. This is a benefit of the strategy already reported by other laboratories.^{15–17,20–22} However, azides are not compatible with the protocol of phosphoramidite chemistry, so postmodification was necessary to introduce the azido group into the

oligonucleotide chain. This reaction uses conventional conjugation chemistry resulting in overall moderate yields.^{20a,32–34} Furthermore, subsequent click reactions are usually limited to terminal positions of an oligonucleotide chain.

As we want to be free in the position of a cross-link and make use of the highly efficient click reaction to link oligonucleotide chains together, our strategy employs bis-azides and oligonucleotides with diynyl chains. If click reactions take place simultaneously at a bis-azide—“bis-click reaction”—only identical oligonucleotide strands

Table 1. T_m Values of Oligonucleotide Duplexes Containing the Modified 8-Aza-7-deaza-2'-deoxyguanosines 1 and 2

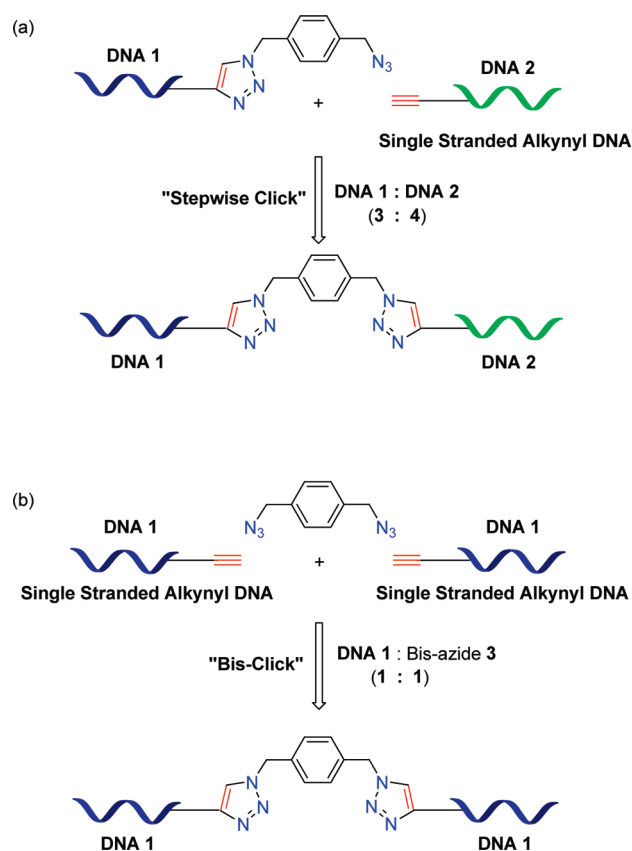
Duplexes	T_m^a [°C]	ΔT_m [°C]	%h ^b	ΔG_{310}^c [kcal/mol]
5'-d(TAG GTC AAT ACT) (ODN-14) 3'-d(ATC CAG TTA TGA) (ODN-15)	51.0	-	18	-11.4
5'-d(TAG GTC AAT ACT) (ODN-14) 3'-d(ATC CA1 TTA TGA) (ODN-16)	53.5	+2.5	17	-12.0
5'-d(TAG GTC AAT ACT) (ODN-14) 3'-d(ATC CAG TTA T1A) (ODN-17)	54.0	+3	15	-12.2
5'-d(TAG 1TC AAT ACT) (ODN-18) 3'-d(ATC CAG TTA TGA) (ODN-15)	53.5	+2.5	16	-12.0
5'-d(TAG GTC AAT ACT) (ODN-14) 3'-d(ATC CA2 TTA TGA) (ODN-19)	51.0	0	15	-11.4
5'-d(TAG GTC AAT ACT) (ODN-14) 3'-d(ATC CAG TTA T2A) (ODN-20)	53.5	+2.5	17	-12.1
5'-d(TAG 2TC AAT ACT) (ODN-21) 3'-d(ATC CAG TTA TGA) (ODN-15)	52.0	+1	18	-11.7

^a Measured at 260 nm in a 1 M NaCl solution containing 100 mM MgCl₂ and 60 mM Na-cacodylate (pH 7.0) with 5 μM + 5 μM single-strand concentration. ^b % h refers to the percentage of hypochromicity. ^c ΔG_{310}^c values are given with 15% error.

Table 2. T_m Values of Duplexes Containing the Monofunctional Derivatives 4 or 5

Duplexes	T_m^a [°C]	ΔT_m [°C]	%h ^b	ΔG_{310}^c [kcal/mol]
5'-d(TAG GTC AAT ACT) (ODN-14) 3'-d(ATC CAG TTA TGA) (ODN-15)	51.0	-	18	-11.4
5'-d(TAG GTC AAT ACT) (ODN-14) 3'-d(ATC CA4 TTA TGA) (ODN-22)	48.0	-3	16	-10.5
5'-d(TAG GTC AAT ACT) (ODN-14) 3'-d(ATC CAG TTA T4A) (ODN-23)	52.0	+1	15	-11.4
5'-d(TAG 4TC AAT ACT) (ODN-24) 3'-d(ATC CAG TTA TGA) (ODN-15)	50.5	-0.5	17	-11.3
5'-d(TAG GTC AAT ACT) (ODN-14) 3'-d(ATC CA5 TTA TGA) (ODN-25)	47.5	-3.5	14	-10.4
5'-d(TAG GTC AAT ACT) (ODN-14) 3'-d(ATC CAG TTA T5A) (ODN-26)	52.0	+1	17	-11.7
5'-d(TAG 5TC AAT ACT) (ODN-27) 3'-d(ATC CAG TTA TGA) (ODN-15)	48.5	-2.5	16	-10.9

^a Measured at 260 nm in a 1 M NaCl solution containing 100 mM MgCl₂ and 60 mM Na-cacodylate (pH 7.0) with 5 μM + 5 μM single-strand concentration. ^b % h refers to percentage of hypochromicity. ^c ΔG_{310}^c values are given with 15% error.

**Figure 2.** Scheme of the "stepwise click" (a) and the "bis-click" (b) reaction.

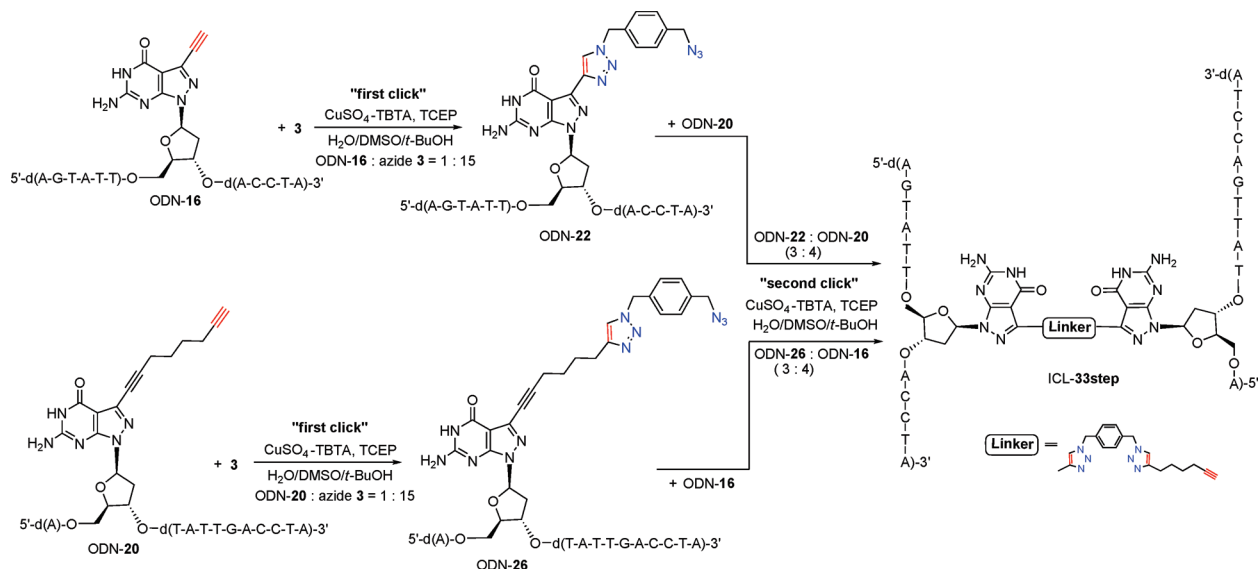
can be ligated selectively. Nonidentical oligonucleotides, being uncomplementary, employed under those conditions give rise to a mixture of various (three) cross-linked products complicating this route greatly. Thus, the "stepwise" protocol was developed which overcomes these limitations. The bis-click and stepwise click strategies are illustrated in Figure 2.

4. Stepwise "Click" Cross-Linking of Oligonucleotides Containing Nucleosides 1 and 2: Cross-Linking between Identical or Nonidentical Strands. The synthetic route of the stepwise click reaction to construct the cross-linked oligonucleotides is shown in Scheme 3, starting with the ethynyl compound ODN-16 or the octadiynyl derivative ODN-20. The click reaction was performed at room temperature in aqueous solution (H₂O/DMSO/*t*-BuOH) employing a premixed 1:1 complex of CuSO₄–TBTA (tris(benzyltriazolylmethyl)amine), TCEP (tris(carboxyethyl)phosphine), and NaHCO₃. NaHCO₃ was essential to complete the reaction within 12 h. The ratio of bis-azide 3 over the respective oligonucleotides was 15:1. With this excess of bis-azide 3 only one azido group reacts ("first click"), thereby yielding the monofunctionalized click intermediates ODN-22 and ODN-26 (Scheme 3 and Table 3). Then, in the second step ("second click"), the intermediates ODN-22 and ODN-26 were reacted with another alkynylated oligonucleotide (ODN-16 or ODN-20) (Scheme 3). The reaction conditions for the second step were the same as those described for the "bis-click" reaction,²³ except that the alkynylated oligonucleotides (ODN-16 or ODN-20) were in slight excess (4:3) over the intermediates ODN-22 and ODN-26. Both routes, using either ODN-16 or ODN-20 as starting material, afforded the identical product ICL-33step.

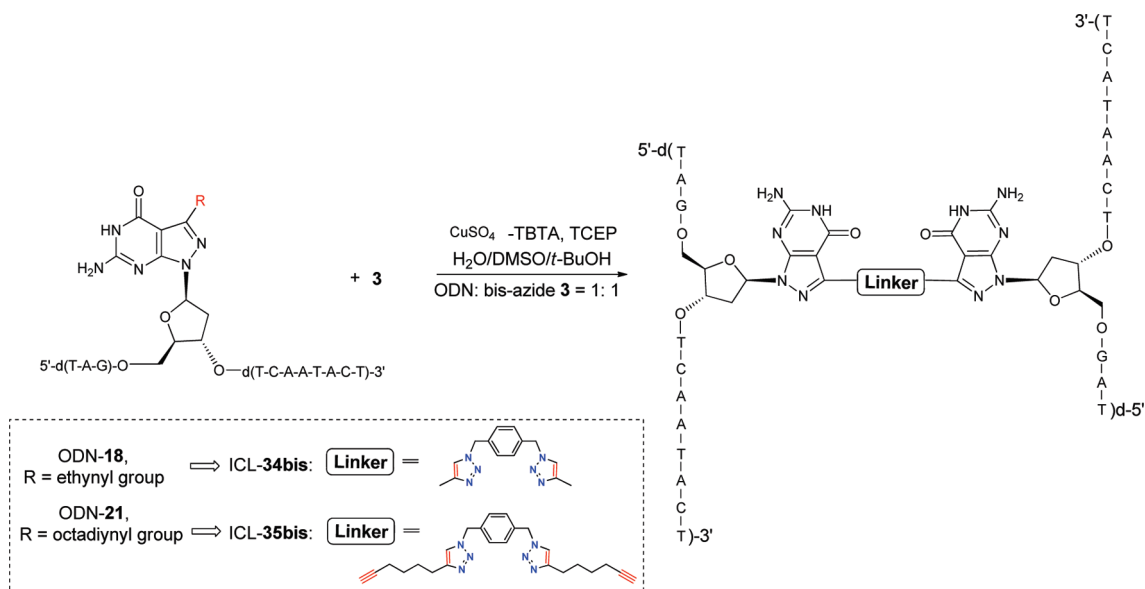
Typical examples for the reversed-phase HPLC profiles of the crude reaction mixtures for selected monofunctionalized intermediates obtained after the "first click" reaction are shown in the Supporting Information (Figure S4a,b). Figure S4e,f (Supporting Information) depicts interstrand cross-linked oligonucleotides obtained after the "second click" reaction. The monofunctionalized oligonucleotides were separated and isolated by reversed-phase HPLC. Moreover, HPLC profiles of mixtures of the ethynyl or octadiynyl compounds and their adducts show that the monofunctionalized intermediates migrate slower than the starting materials but faster than the cross-linked oligonucleotides (Figure S3, Supporting Information).

We were able to start the stepwise click reaction with various oligonucleotides (ODN-16–ODN-21) with short or long linkers and various linking positions affording monoazide

Scheme 3. Interstrand Cross-linking of Oligonucleotides by the Cu(I)-Catalyzed “Stepwise Click” Reaction Using Oligonucleotide ODN-16 (Short Linker) or ODN-20 (Long Linker) in the “First Click” and Oligonucleotide ODN-20 (Long Linker) or ODN-16 (Short Linker) in the “Second Click”



Scheme 4. Interstrand Cross-Linking of Oligonucleotides ODN-18 and ODN-21 by Cu(I)-Catalyzed “Bis-click” Reaction



intermediates ODN-22–ODN-27 (Table 3 and Figures S5–S7, Supporting Information). The monofunctionalized oligonucleotides were always completely consumed while the remaining excess of the alkynylated oligonucleotides was still seen in the HPLC profiles. The cross-linked oligonucleotides were separated and purified by reversed-phase HPLC (RP-18 column) (Figures S5–S7, Supporting Information). Accordingly, a series of cross-linked oligonucleotides (ICL-28step–ICL-33step) as shown in Table 3 were prepared. All oligonucleotide conjugates were characterized by LC-ESI-TOF or MALDI-TOF mass spectrometry (Table S3, Supporting Information); even oligonucleotides bearing azido groups did not decompose during mass spectrometry and gave the expected molecular weights in all cases.

Table 3 summarizes the various cross-linked oligonucleotides ICL-28step–ICL-33step as well as the oligonucleotide intermediates still carrying one azido group (ODN-22–ODN-27) obtained from the “stepwise click” reaction. The cross-linked oligonucleotides are composed of (i) identical strands or (ii) nonidentical strands employing a combination of (iii) two short or (iv) two long linkers as well as (v) a combination of a long and a short linker. The linking positions are placed at (vi) a central or (vii) a terminal position. The diversity of possible combinations demonstrates the powerful potential of the “stepwise click” reaction as the three parameters oligonucleotide sequence, linker length, and linking position can be varied freely.

Table 3. Oligonucleotide Intermediates with Azido Groups and Cross-linked Oligonucleotides with Identical and Nonidentical Strands Prepared by the “Stepwise Click” Reaction with Different Linking Positions and Linkers of Different Length^a

ODN intermediates with azido groups	Linker (chain type)	ODN intermediates with azido groups	Linker (chain type)
5'-d(AGT ATT 4 AC CTA) (ODN-22)	Short	5'-d(AGT ATT 5 AC CTA) (ODN-25)	Long
5'-d(A4 T ATT GAC CTA) (ODN-23)	Short	5'-d(A5 T ATT GAC CTA) (ODN-26)	Long
5'-d(TAG 4 TC AAT ACT) (ODN-24)	Short	5'-d(TAG 5 TC AAT ACT) (ODN-27)	Long
Cross-linked oligonucleotides	Linker (length and position)	Cross-linked oligonucleotides	Linker (length and position)
5'-d(AGT ATT 1 AC CTA) 5'-d(AGT ATT 1 AC CTA) (ICL-28step)	Short-Short (C-C)	5'-d(AGT ATT 1 AC CTA) 5'-d(A1 T ATT GAC CTA) (ICL-32step)	Short-Short (C-T)
5'-d(A1 T ATT GAC CTA) 5'-d(A1 T ATT GAC CTA) (ICL-29step)	Short-Short (T-T)	5'-d(AGT ATT 1 AC CTA) 5'-d(A2 T ATT GAC CTA) (ICL-33step) ^b	Short-Long (C-T)
5'-d(AGT ATT 2 AC CTA) 5'-d(AGT ATT 2 AC CTA) (ICL-30step)	Long-Long (C-C)	5'-d(AGT ATT 1 AC CTA) 5'-d(A2 T ATT GAC CTA) (ICL-33step) ^c	Short-Long (C-T)
5'-d(A2 T ATT GAC CTA) 5'-d(A1 T ATT GAC CTA) (ICL-31step)	Long-Short (T-T)		

^a 1-1, 2-2, 1-2, and 2-1 represent the cross-linked nucleosides formed by the cycloaddition of the azido group within one side chain and the terminal triple bond of the other side chain. For detailed structures see Figure S2, Supporting Information. The various connectivities are as follows: C–C central position connected with central position; T–T terminal position connected with terminal position; C–T central position connected with terminal position.

Table 4. Cross-Linked Oligonucleotides with Identical Strands Prepared by the “Bis-click” Reaction with Identical Linker Length^a

Cross-linked oligonucleotides	Linker (length and position)	Cross-linked oligonucleotides	Linker (length and position)
5'-d(AGT ATT 1 AC CTA) 5'-d(AGT ATT 1 AC CTA) (ICL-28bis)	Short-Short (C-C)	5'-d(AGT ATT 2 AC CTA) 5'-d(AGT ATT 2 AC CTA) (ICL-30bis)	Long-Long (C-C)
5'-d(TAG 1 TC AAT ACT) 5'-d(TAG 1 TC AAT ACT) (ICL-34bis)	Short-Short (C-C)	5'-d(TAG 2 TC AAT ACT) 5'-d(TAG 2 TC AAT ACT) (ICL-35bis)	Long-Long (C-C)
5'-d(A1 T ATT GAC CTA) 5'-d(A1 T ATT GAC CTA) (ICL-29bis)	Short-Short (T-T)	5'-d(A2 T ATT GAC CTA) 5'-d(A2 T ATT GAC CTA) (ICL-36bis)	Long-Long (T-T)

^a 1-1 or 2-2 represent the cross-linked nucleosides formed by the cycloaddition of the azido group within one side chain and the terminal triple bond of the other side chain. For detailed structures see Figure S2, Supporting Information. The various connectivities are: C–C central position connected with central position; T-T terminal position connected with terminal position.

The hybridization of oligonucleotides incorporating the azido intermediates **4** or **5** with complementary oligonucleotide strands results into slightly reduced T_m values compared to the parent alkylnylated oligonucleotide duplexes. Modifications at central positions have a stronger destabilizing effect (about -3 °C) than at terminal positions (around $+1$ °C). These findings are in line with previous observations on side-chain modifications reporting on duplex destabilization when the side chain gets too long.^{27a-c} For further details, see Table 2.

The “stepwise click reaction” can also be carried out on oligonucleotides with identical strands leading to the same reaction products as obtained from the “bis-click reaction”. Both reactions were performed in order to compare the cross-linked reaction products of both protocols. Indeed, the stepwise click and the bis-click reaction (Scheme 4) yielded identical cross-linked oligonucleotides as demonstrated on ICL-28step, ICL-29step, ICL-30step (Table 3) and ICL-28bis, ICL-29bis, ICL-30bis (Table 4). For hybridization studies, the cross-linked

oligonucleotides ICL-34bis–ICL-36bis were also prepared by the bis-click reaction (Table 4). Although the reaction is template-free, it proceeds smoothly forming the bis-click products as major compounds (major peaks; ICL-34bis and ICL-35bis; Figure S8, Supporting Information). Only a small amount (minor peaks) of the respective monofunctionalized oligonucleotides still carrying one azido group (ODN-24 and ODN-27) were detected as shown in the reversed-phase HPLC profiles (RP-18 column) of the crude reaction mixtures. The starting material which migrates faster than the cross-linked or monofunctionalized oligonucleotides was completely consumed. The contents of the major peaks containing ICL-34bis and ICL-35bis were separated by HPLC and isolated. The formation of cross-linked oligonucleotides was further confirmed by the molecular masses of the final reaction products determined by LC-ESI-TOF and MALDI-TOF mass spectrometry (Supporting Information, Table S4).

Comparing the protocols of the bis-click and stepwise click reaction, it can be concluded that for the synthesis of cross-linked oligonucleotides with identical strands, the protocol of the bis-click reaction is advantageous over the stepwise click reaction affording cross-linked oligonucleotides with yields in the range of 50–70%. The stepwise click reaction requires the isolation of the monofunctionalized intermediate. Thus, the overall yield over two steps is generally lower (step 1, about 60–80%; step 2, about 40–50%). However, for the synthesis of cross-linked oligonucleotides with nonidentical strands the stepwise click protocol represents a versatile method.

Finally, ion-exchange chromatography was performed with the starting materials and products of the stepwise-click and the bis-click reaction (Figure 3). ODN-16 and ODN-22 show almost identical retention times (11.5 and 12.2 min) because of 11 negative phosphate charges (Figure 3a), while the retention time of the cross-linked ICL-28step is increased by 6 min (22 negative phosphate charges). The retention time of cross-linked ICL-28step is almost identical to the retention time of the duplex 14·15³⁵ as the number of charges of the cross-linked oligonucleotide is doubled compared to the non-cross-linked oligonucleotides ODN-16 and ODN-22. Mobility shift analysis was also carried out for the bis-click reaction of ODN-20 affording ICL-36bis (Figure 3b).

5. Influence of DNA Interstrand Cross-Links on Oligonucleotide Duplex Stability. The cross-linked oligonucleotides of Tables 3 and 4 gave us the opportunity to construct DNA assemblies by a combination of cross-linking and hybridization which generated DNA structures with novel structural features. For this, cross-linked oligonucleotides were hybridized with individual complementary strands to form two double-stranded helices covalently linked by the cycloadduct of the alkylnyl side chains and the azido groups. Herein, a pyrazolo[3,4-*d*]pyrimidine base related to guanine was used as nucleobase at the modification sites. The linkers which were always connected to the 7-position of the 8-aza-7-deazaguanine moiety were changed in length and position. Cross-linked oligonucleotides of identical and nonidentical strands were studied. Also, cross-linked strands were hybridized with the corresponding complementary cross-linked species. However, 7-substituted 7-deazapurines or 5-substituted pyrimidines related to the canonical DNA bases or even universal bases and other residues can be used for this purpose.

A related strategy using the phosphodiester backbone as connecting point was reported by Endo et al.³⁶ However, this method removed the negative charge from the internucleotide phosphodiester linkage and generated *R_p* and *S_p* diastereoisomers which had to be separated. This resulted in a dramatic *T_m* decrease. In the work of Endo et al., only identical strands were ligated, and disulfide formation was used for cross-linking.³⁶

We started our hybridization studies with cross-linked oligonucleotides with two identical strands. They were hybridized with individual complementary chains to give cross-linked double-stranded helices. *T_m* measurements of 2.5 μM of cross-linked DNA and 5 μM of the single-stranded complementary oligonucleotides (ODN-14 or ODN-15) were performed. Then, the influence of the linker length and position was evaluated. As shown in Table 5, the duplex stability varies according to the position of the cross-linker. When positioning a short linker (combination of two ethynyl side chains) at a central position, the *T_m* value decreases by 17 °C (14·ICL-28step·14) or 10 °C (15·ICL-34bis·15) compared to the reference duplex 14·15. On the contrary, the destabilization is almost negligible

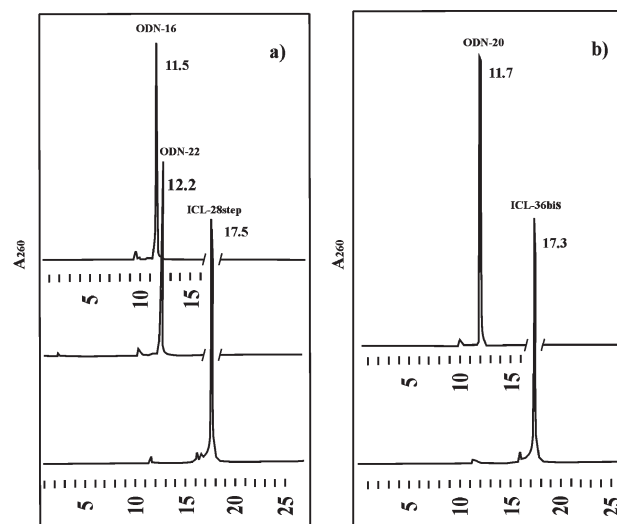


Figure 3. Ion-exchange HPLC elution profiles of (a) oligonucleotide ODN-16, azidomethylbenzyl-labeled ODN-22, and the interstrand cross-linked ICL-28step. (b) Oligonucleotide ODN-20 and the interstrand cross-link ICL-36bis on a 4 × 250 mm DNA PA-100 column using the following buffer system: (C) 25 mM Tris-HCl, 10% MeCN, pH 7.0; (D) 25 mM Tris-HCl, 1.0 M NaCl, and 10% MeCN, pH 7.0. Elution gradient IV: 0–30 min 20–80% D in C with a flow rate of 0.75 mL min⁻¹.

(14·ICL-29step·14: $\Delta T_m = -1.5$ °C) for a short cross-link at a terminal position.

A similar observation is made when the linker is longer (combination of two octadiynyl chains). However, in this case, the *T_m* decrease is significantly reduced compared to duplexes with short linkers (34.0 °C for 14·ICL-28step·14 vs 45.0 °C for 14·ICL-30step·14 or 41.0 °C for 15·ICL-34bis·15 vs 47.0 °C for 15·ICL-35bis·15; central positions). For the terminal cross-linking position, even a small stabilization over the reference duplex 14·15 was observed (14·ICL-36bis·14: $\Delta T_m = +1.0$ °C).

The *T_m* value of duplex 14·ICL-31step·14 with a combination of a short (ethynyl) and a long (octadiynyl) linker introduced at a terminal position is even more stable ($\Delta T_m = +2.0$ °C).

In addition, we cross-linked oligonucleotides at a central position of one strand and at a terminal position of the other strand. For this, we used a combination of two ethynyl linkers (14·ICL-32step·14) or of an ethynyl and octadiynyl linker (14·ICL-33step·14). As shown in Table 5, duplex 14·ICL-33step·14 (*T_m* = 48.5 °C) is significantly more stable than 14·ICL-32step·14 with two short linkers (*T_m* = 45.0 °C).

Next, two linker units were introduced in the cross-linked duplexes. This was realized by hybridizing a cross-linked species with identical strands with a second cross-linked species also with identical strands but with complementary base sequence (duplexes ICL-34·ICL-28 and ICL-35·ICL-28; Table 5 and Figure 4c, d). Now, the *T_m* values increased significantly over those of the cross-linked duplexes with only one cross-link (56.0 °C for ICL-34·ICL-28 with two cross-links vs 41.0 °C for 15·ICL-34bis·15 and 34.0 °C for 14·ICL-28step·14, each with one cross-link). As the cross-links were introduced near the central position, the effect of double cross-linking over the single cross-linking is rather strong with a *T_m* increase of 15 or 22 °C.

Table 5. T_m Values of Cross-Linked Oligonucleotides ICL-28–ICL-35 Prepared by the “Stepwise Click” and the “Bis-click” Reaction

Interstrand Cross-linked Duplexes	T_m^a [°C]	ΔT_m [°C]	%h ^b	Interstrand Cross-linked Duplexes	T_m^a [°C]	ΔT_m [°C]	%h ^b
5'-d(TAG GTC AAT ACT) (ODN-14) 3'-d(ATC CAG TTA TGA) (ODN-15)	51.0 (47.5)	-	18 (16)				
5'-d(TAG GTC AAT ACT) (ODN-14) 3'-d(ATC CA1 TTA TGA) 3'-d(ATC CA1 TTA TGA) 5'-d(TAG GTC AAT ACT) (ODN-14) (ICL-28step)	34.0	-17	8	5'-d(TAG GTC AAT ACT) (ODN-14) 3'-d(ATC CAG TTA T1A) 3'-d(ATC CAG TTA T1A) 5'-d(TAG GTC AAT ACT) (ODN-14) (ICL-29step)	49.5	-1.5	15
5'-d(TAG GTC AAT ACT) (ODN-14) 3'-d(ATC CA2 TTA TGA) 3'-d(ATC CA2 TTA TGA) 5'-d(TAG GTC AAT ACT) (ODN-14) (ICL-30step)	45.0 (42.0)	-6 (-5.5)	14 (15)	5'-d(TAG GTC AAT ACT) (ODN-14) 3'-d(ATC CAG TTA T1A) 3'-d(ATC CAG TTA T2A) 5'-d(TAG GTC AAT ACT) (ODN-14) (ICL-31step)	53.0	+2.0	20
5'-d(TAG GTC AAT ACT) (ODN-14) 3'-d(ATC CA1 TTA TGA) 3'-d(ATC CAG TTA T1A) 5'-d(TAG GTC AAT ACT) (ODN-14) (ICL-32step)	45.0	-6	12	5'-d(TAG GTC AAT ACT) (ODN-14) 3'-d(ATC CA1 TTA TGA) 3'-d(ATC CAG TTA T2A) 5'-d(TAG GTC AAT ACT) (ODN-14) (ICL-33step)	48.5	-2.5	15
3'-d(ATC CAG TTA TGA) (ODN-15) 5'-d(TAG 1TC AAT ACT) 5'-d(TAG 1TC AAT ACT) 3'-d(ATC CAG TTA TGA) (ODN-15) (ICL-34bis)	41.0	-10	12	3'-d(ATC CAG TTA TGA) (ODN-15) 5'-d(TAG 2TC AAT ACT) 5'-d(TAG 2TC AAT ACT) 3'-d(ATC CAG TTA TGA) (ODN-15) (ICL-35bis)	47.0	-4.0	16
5'-d(TAG GTC AAT ACT) (ODN-14) 3'-d(ATC CAG TTA T2A) 3'-d(ATC CAG TTA T2A) 5'-d(TAG GTC AAT ACT) (ODN-14) (ICL-36bis)	52.0	+1	21				
5'-d(TAG 1 TC AAT ACT) (ICL-34) 3'-d(ATC 1 CA1 TTA TGA) (ICL-28) 3'-d(ATC 1 CA1 TTA TGA) (ICL-28) 5'-d(TAG 1 TC AAT ACT) (ICL-34)	56.0 (52.0)	+5 (+4.5)	12 (12)	5'-d(TAG 2 TC AAT ACT) (ICL-35) 3'-d(ATC 1 CA1 TTA TGA) (ICL-28) 3'-d(ATC 1 CA1 TTA TGA) (ICL-28) 5'-d(TAG 2 TC AAT ACT) (ICL-35)	53.5	+2.5	11

^a Measured at 260 nm in a 1 M NaCl solution containing 100 mM MgCl₂ and 60 mM Na-cacodylate (pH 7.0) with 2.5 μM of cross-linked DNA and 5 μM of the single-stranded complementary oligonucleotides. 1-1, 2-2, 1-2, or 2-1 represent the cross-linked nucleosides formed by the cycloaddition of the azido group within one side chain and the terminal triple bond of the other side chain. For structural details of the cross-linked oligonucleotides, see Figure S2, Supporting Information. Data in parentheses refer to measurements in 0.1 M NaCl, 10 mM MgCl₂, 10 mM Na-cacodylate, pH 7.0. ^b % h refers to percentage of hypochromicity.

The stability of these double cross-linked duplexes is also spacer depended. A combination of two short linkers (ethynyl–ethynyl; ICL-34·ICL-28: T_m = 56.0 °C) is more favorable than a combination of a short and long linker (ethynyl–ethynyl and octadiynyl–octadiynyl; ICL-35·ICL-28: T_m = 53.5 °C). The stability of the double cross-linked duplexes is even higher than that of the parent noncross-linked duplex 14·15. This results from an entropically more favorable situation for duplexes formed by two complementary cross-linked strands compared to duplexes formed by only one cross-linked strand and two individual strands. The details of the various combinations and their influence on the duplex stability are listed in Table 5.

The various types of cross-linked duplexes were modeled with Hyperchem 8.0 (Hypercube Inc.) without energy minimization. Sphere models are shown in Figure 4. In all cases, the side linkers protrude into the major groove of B-DNA. It is expected that the double helix geometry should not be affected significantly when linker arms are positioned in such uncritical positions, e.g., the 7-position of the 8-aza-7-deazaguanine bases, even when rather short linkers or two linkers units are introduced. Nevertheless, as indicated by the decrease of T_m values (Table 5), cross-linking in central positions affects duplex stability. Many factors can account

for this phenomenon: (i) distortion of the helix, (ii) changes in helix hydration by water molecules, (iii) hydrophobic effects caused by the lipophilic linker, etc. Apparently, all these unfavorable properties can be superimposed by the entropic gain induced by the cross-linking of oligonucleotide chains in particular, when each individual complementary species is cross-linked before hybridization.

CONCLUSIONS AND OUTLOOK

Various DNA cross-linking methods have already been reported, including the so-called “bis-click” protocol.^{1,37–40} While the application of the template-independent “bis-click” reaction is limited to identical oligonucleotide strands, we developed the “stepwise click” methodology which allows us to cross-link any oligonucleotide bearing an alkynyl linker as a side chain in a selective way with a bis-azide. For this, alkynylated 8-aza-7-deaza-2'-deoxyguanine residues with short and long linker arms (1 and 2) were incorporated into a series of 12-mer oligodeoxyribonucleotides (ODNs) using solid-phase synthesis and employing phosphoramidites 12 and 13. The stepwise click methodology requires an excess of the bis-azide over the modified

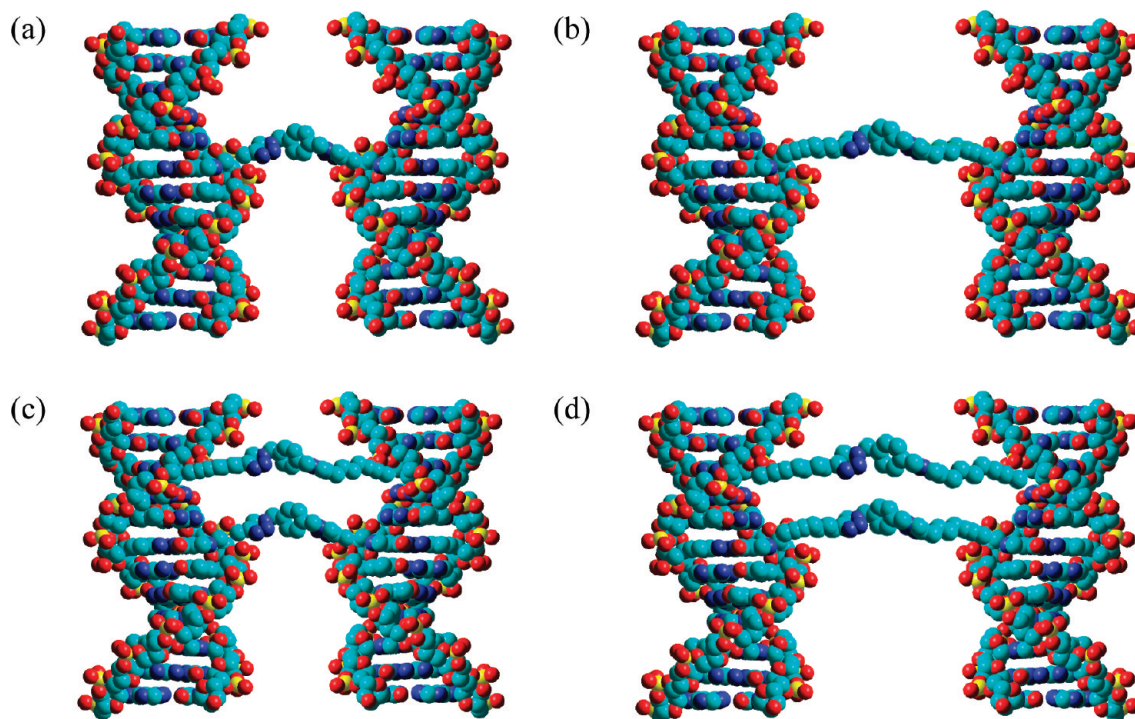


Figure 4. Schematic representations of the molecular models of two double helices connected by (a) the short linker and (b) by a long linker, both in a central position of the helix and (c) with a short linker in a central and a long linker in a near terminal position and (d) with two long linkers in terminal and central positions. The models were constructed using Hyperchem 8.0.

oligonucleotide and yields a monofunctionalized intermediate which still carries one reactive azido group. These oligonucleotides were then cross-linked in a second click reaction with the terminal triple bond of a second oligonucleotide in a selective way. Homocoupling of identical strands is excluded. By this route, cross-linked oligonucleotides are accessible having the cross-link at any position of the chain with linker arms of various lengths. Also, the linking positions can be varied freely.

We have hybridized the various cross-linked oligonucleotides with complementary oligonucleotides including those which were already cross-linked before. As in the functionalized molecules the linker protrudes into the major groove of the DNA, only small distortions of the duplex structures were expected. Indeed, stable cross-linked duplexes were formed with short and long linker arms as displayed in Figure 4a,b. Nevertheless, cross-linking near terminal positions using long linkers results in more stable helices than those modified near or at the center of duplex DNA with a short linker. We anticipate that our methodology might find broad application in chemical biology and the construction of nanostructures. Also, the stepwise click method can be applied for other molecules including natural biopolymers such as carbohydrates or polypeptides or in material science.^{41–47} Currently, the stepwise click reaction is studied on solid-phase in order to simplify the two-step protocol. Also, we were able to show that a template-controlled bis-click reaction can be performed in a selective way when complementary oligonucleotide strands are ligated with bis-azides within a duplex structure.

EXPERIMENTAL SECTION

General Methods. All chemicals and solvents were of laboratory grade as obtained from commercial suppliers and were used without

further purification. Thin-layer chromatography (TLC) was performed on TLC aluminum sheets covered with silica gel 60 F254 (0.2 mm). Flash column chromatography (FC): silica gel 60 (40–60 μM) at 0.4 bar. UV spectra: λ_{max} in nm, ϵ in $\text{dm}^3 \text{mol}^{-1} \text{cm}^{-1}$. NMR spectra: measured at 300.15 MHz for ^1H , 75.48 MHz for ^{13}C and 121.52 MHz for ^{31}P . The J values are given in Hz and δ in ppm. For NMR spectra recorded in DMSO, the chemical shift of the solvent peak was set to 2.50 ppm for ^1H NMR and 39.50 ppm for ^{13}C NMR (see Table 6). Reversed-phase HPLC was carried out on a 250×4 mm RP-18 LiChrospher 100 column with a HPLC pump connected with a variable wavelength monitor, a controller and an integrator. Gradients used for HPLC chromatography: A = MeCN; B = 0.1 M $(\text{Et}_3\text{NH})\text{OAc}$ (pH 7.0)/MeCN, 95:5. Conditions: (I) 3 min 15% A in B, 12 min 15–50% A in B, and 5 min 50–10% A in B, flow rate 0.7 mL min^{-1} ; (II) 0–25 min 0–20% A in B, flow rate 0.7 mL min^{-1} ; (III) 0–15 min 0–20% A in B, 15–18 min 20–40% A in B, flow rate 0.7 mL min^{-1} . ESI-TOF mass spectra of the nucleosides and oligonucleotides were measured with a Micro-TOF spectrometer. Molecular mass of oligonucleotides were determined by LC-ESI-TOF mass spectrometry or by MALDI-TOF mass spectrometry in the linear negative mode with 3-hydroxypicolinic acid (3-HPA) as a matrix. The detected masses were in line with the calculated values (Tables S2–S4, Supporting Information).

Synthesis, Purification, and Characterization of Oligonucleotides. The syntheses of oligonucleotides were performed on a DNA synthesizer at a $1 \mu\text{mol}$ scale (trityl-on mode) using the phosphoramidite 12 or 13 and the standard phosphoramidite building blocks following the synthesis protocol for 3'-O-(2-cyanoethyl)phosphoramidites.⁴⁸ After cleavage from the solid support, the oligonucleotides were deprotected in 25% aqueous ammonia solution for 12–16 h at 60 $^\circ\text{C}$. The purification of the "trityl-on" oligonucleotides was carried out on reversed-phase HPLC (RP-18 column; gradient system I). The purified "trityl-on" oligonucleotides were treated with 2.5% of $\text{Cl}_2\text{CHCOOH}/\text{CH}_2\text{Cl}_2$ for 5 min at 0 $^\circ\text{C}$ to remove the 4,4'-dimethoxytrityl residues.

Table 6. ^{13}C -NMR Chemical Shifts of 8-Aza-7-deaza-2'-deoxyguanosine Derivatives^a

	C(2) ^b C(6) ^c	C(4) ^b C(7a) ^c	C(5) ^b C(3a) ^c	C(6) ^b C(4) ^c	C(7) ^b C(3) ^c	C≡C	triazole	C(1')	C(2')	C(3')	C(4')	C(5')
1	155.6 ^d	155.4 ^d	83.8	157.0 ^d	129.2	100.4, 75.9		83.3	38.7	70.9	87.6	62.4
9	155.5 ^d	155.3 ^d	88.9	156.8 ^d	129.5	100.3, 97.0		83.2	38.7	70.9	87.5	62.3
10	158.8 ^d	154.7 ^d	84.0	159.7 ^d	129.3	102.9, 76.0		83.5	38.7	71.1	87.7	62.5
11	158.7 ^d	154.6 ^d	83.8	159.5 ^d	129.6	102.9, 76.1		83.1	38.7	70.5	85.3	64.1
4	156.3 ^d	155.0 ^d	96.6	158.0 ^d	138.4		125.8, 139.9	83.2	38.7	71.1	87.6	62.5
5	155.5 ^d	155.2 ^d	93.4	157.1 ^d	130.4	100.0, 73.1	122.1, 147.1	83.1	38.7	71.0	87.5	62.4
6	156.3 ^d	155.0 ^d	96.6	158.0 ^d	138.4		125.8, 139.9	83.2	38.7	71.1	87.6	62.5
7 ²³	155.5 ^d	155.2 ^d	93.4	157.1 ^d	130.4	100.0, 73.1	122.1, 147.0	83.1	38.6	70.9	87.5	62.4

^a Measured in DMSO-*d*₆ at 298 K. ^b Purine numbering. ^c Systematic numbering. ^d Tentative.

The detritylated oligomers were purified by reversed-phase HPLC (gradient II). The oligomers were desalted on a short column using distilled water for elution of salt, while the oligonucleotides were eluted with H₂O/MeOH (2:3). Then, the solvent was evaporated using a SpeedVac evaporator to yield colorless solids which were frozen at -24 °C. The molecular masses of the oligonucleotides were determined by LC-ESI-TOF mass spectrometry or by MALDI-TOF mass spectrometry in the linear negative mode (for spectra, see Figures S12–S27, Supporting Information).

Ion-Exchange HPLC Analysis of DNA Interstrand Cross-Linked Oligonucleotides. Mobility Shift Analyses. The ion-exchange chromatography was performed on a 4 × 250 mm DNA PA-100 column with a precolumn using a HPLC apparatus. Elution profiles were recorded at 260 nm. The alkynylated oligonucleotides ODN-16, ODN-20, azidomethylbenzyl-labeled ODN-22 and interstrand cross-linked oligonucleotides ICL-28step and ICL-36bis (0.1 A₂₆₀ units each) were dissolved in 100 μL of water and then directly injected into the apparatus. The compounds were eluted using gradient IV: 0–30 min with 20–80% D in C with a flow rate of 0.75 mL min⁻¹ ((C) 25 mM Tris-HCl, 10% MeCN, pH 7.0; (D) 25 mM Tris-HCl, 1.0 M NaCl, 10% MeCN, pH 7.0).

T_m Measurements. The oligonucleotides were dissolved in 1 M NaCl, 100 mM MgCl₂, and 60 mM Na-cacodylate buffer, pH 7.0 or 100 mM NaCl, 10 mM MgCl₂ and 10 mM Na-cacodylate, pH 7.0. For non-cross-linked oligonucleotide duplexes 5 μM + 5 μM single-stranded concentration was used. Hybridization experiments to obtain cross-linked duplexes were carried out with 2.5 μM of the cross-linked oligonucleotide and 5 μM of the complementary non-cross-linked oligonucleotide. Hybridization experiments to obtain double cross-linked duplexes were carried out with 2.5 μM of each cross-linked oligonucleotide.

The melting temperature curves were measured with a UV–vis spectrophotometer equipped with a thermoelectrical controller. The temperature was measured continuously in the reference cell with a Pt-100 resistor with a heating rate of 1 °C min⁻¹, and the absorbance at 260 nm was recorded as a function of the temperature. The thermodynamic data of duplex formation were calculated by the MeltWin (version 3.0) program using the curve fitting of the melting profiles according to a two-state model.⁴⁹

The hypochromicity (*h* (%)) = [(E_{monomer} - E_{polymer})/(E_{monomer})⁻¹]-100%) of the oligonucleotides was determined from the melting curves. The extinction coefficients of the oligonucleotides were calculated from the sum of the extinction coefficients of the monomeric 2'-deoxyribonucleosides divided by the hyperchromicity.⁵⁰ Extinction coefficients ε₂₆₀ (MeOH) of the nucleosides: dA 15400, dG 11700, dT 8800, dC 7300, 1 10900, 2 11500, 4 26000, 5 23100, 6 31800 (0.1 M aq NaOH), 7 23000.

6-Amino-1-(2-deoxy-β-D-erythro-pentofuranosyl)-1,5-dihydro-3-[2-(trimethylsilyl)ethynyl]-4H-pyrazolo[3,4-d]pyrimidin-4-one (9). A solution of 8³¹ (1.2 g, 3.0 mmol) in dry DMF

(15 mL) was treated with CuI (120 mg, 0.6 mmol), [Pd⁰[P(Ph₃)₄] (360 mg, 0.3 mmol), anhydrous Et₃N (220 μL, 3.0 mmol), and 7.0 equiv of (trimethylsilyl)acetylene (2.06 g, 21.0 mmol). The reaction mixture was stirred under N₂ for 2 days (TLC monitoring). The mixture was diluted with MeOH/CH₂Cl₂, 1:1 (60 mL), and Dowex HCO₃⁻ (100 ± 200 mesh; 3.0 g) was added. After the mixture was stirred for 15 min, the evolution of gas ceased. Stirring was continued for another 30 min, and the resin was filtered off and washed with MeOH/CH₂Cl₂, 1:1 (200 mL). The combined filtrate was evaporated, and the oily residue was adsorbed on silica gel and loaded on the top of a column. FC (silica gel, column 15 × 3 cm, eluted with CH₂Cl₂/MeOH, 95:5 → 90:10) afforded one main zone. Evaporation of the solvent furnished 9 as a colorless foam (760 mg, 68%): TLC (CH₂Cl₂/MeOH, 90:10) R_f 0.75; λ_{max} (MeOH)/nm 246 (ε/dm³ mol⁻¹ cm⁻¹ 28400), 260 (15800), 280 (6000); ¹H NMR (DMSO-*d*₆, 300 MHz) (δ, ppm) 0.24 (s, 9H, 3 × CH₃), 2.10–2.18 (m, 1H, 2'-H_α), 2.61–2.69 (m, 1H, 2'-H_β), 3.42–3.50 (m, 2H, 5'-H₂), 3.73–3.78 (m, 1H, 4'-H), 4.31–4.37 (m, 1H, 3'-H), 4.74 (t, J = 5.7 Hz, 1H, 5'-OH), 5.24–5.25 (d, J = 4.2 Hz, 1H, 3'-OH), 6.27 (t, J = 6.6 Hz, 1H, 1'-H), 6.77 (br s, 2H, NH₂), 10.72 (s, 1H, NH). Anal. Calcd. for C₁₅H₂₁N₅O₄Si (363.44): C, 49.57; H, 5.82; N, 19.27. Found: C, 49.61; H, 5.76; N, 19.10.

6-Amino-1-(2-deoxy-β-D-erythro-pentofuranosyl)-1,5-dihydro-3-ethynyl-4H-pyrazolo[3,4-d]pyrimidin-4-one (1). A solution of compound 9 (650 mg, 1.79 mmol) and anhyd K₂CO₃ (160 mg, 1.16 mmol) in MeOH (40 mL) was stirred for 6 h at rt. After evaporation, the residue was adsorbed on silica gel and loaded on the top of a column. FC (silica gel, column 15 × 3 cm, eluted with CH₂Cl₂/MeOH, 95:5 → 90:10 → 85:15) afforded one main zone. The isolated product was recrystallized from MeOH, and 1 (430 mg, 83%) was obtained as a colorless solid: TLC (CH₂Cl₂/MeOH, 80:20) R_f 0.47; λ_{max} (MeOH)/nm 240 (ε/dm³ mol⁻¹ cm⁻¹ 24500), 260 (10900), 280 (5800); ¹H NMR (DMSO-*d*₆, 300 MHz) (δ, ppm) 2.08–2.19 (m, 1H, 2'-H_α), 2.60–2.69 (m, 1H, 2'-H_β), 3.43–3.51 (m, 2H, 5'-H₂), 3.73–3.78 (m, 1H, 4'-H), 4.34–4.38 (m, 2H, 3'-H, C≡CH), 4.73 (t, J = 5.4 Hz, 1H, 5'-OH), 5.23–5.25 (d, J = 4.2 Hz, 1H, 3'-OH), 6.28 (t, J = 6.6 Hz, 1H, 1'-H), 6.79 (br s, 2H, NH₂), 10.79 (s, 1H, HN). Anal. Calcd for C₁₂H₁₃N₅O₄ (291.10): C, 49.48; H, 4.50; N, 24.04. Found: C, 49.35; H, 4.52; N, 23.91.

6-[[Dimethylamino)methylidene]amino]-1-(2-deoxy-β-D-erythro-pentofuranosyl)-1,5-dihydro-3-ethynyl-4H-pyrazolo[3,4-d]pyrimidin-4-one (10). To a solution of compound 1 (592 mg, 2.0 mmol) in MeOH (20 mL) was added *N,N*-dimethylformamide dimethyl acetal (7 mL, 50.0 mmol). The mixture was stirred for 2 h at rt. The solvent was evaporated, and the residue was applied to FC (silica gel, column 15 × 3 cm, eluted with CH₂Cl₂/MeOH, 95:5 → 90:10). Evaporation of the main zone afforded 10 as colorless foam (560 mg, 80%): TLC (CH₂Cl₂/MeOH, 90:10) R_f 0.40; λ_{max} (MeOH)/nm 246 (ε/dm³ mol⁻¹ cm⁻¹ 17500), 255 (21700), 300 (21400); ¹H NMR (DMSO-*d*₆, 300 MHz) (δ, ppm) 2.18–2.22 (m, 1H, 2'-H_α), 2.63–2.72

(m, 1H, 2'-H_β), 3.05 (s, 3H, NCH₃), 3.18 (s, 3H, NCH₃), 3.42–3.50 (m, 2H, 5'-H₂), 3.76–3.81 (m, 1H, 4'-H), 4.38–4.40 (m, 2H, 3'-H, C≡CH), 4.76 (t, *J* = 5.7 Hz, 1H, 5'-OH), 5.30–5.31 (d, *J* = 4.2 Hz, 1H, 3'-OH), 6.45 (t, *J* = 6.3 Hz, 1H, 1'-H), 8.67 (s, 1H, N=CH), 11.36 (s, 1H, HN). Anal. Calcd for C₁₅H₁₈N₆O₄ (346.14): C, 52.02; H, 5.24; N, 24.27. Found: C, 52.54; H, 5.16; N, 24.46.

6-[[[(Dimethylamino)methylidene]amino]-1-[2-deoxy-5-O-(4,4'-dimethoxytriphenylmethyl)-β-D-erythro-pentofuranosyl]-1,5-dihydro-3-ethynyl-4H-pyrazolo[3,4-d]pyrimidin-4-one (11). Compound 10 (550 mg, 1.6 mmol) was dried by repeated coevaporation with anhydrous pyridine and then dissolved in dry pyridine (15 mL) and stirred with 4,4'-dimethoxytrityl chloride (810 mg, 2.4 mmol) in the presence of *N,N*-diisopropylethylamine (430 μL, 2.4 mmol) at room temperature. After 6 h, the solution was poured into 5% aqueous NaHCO₃ (100 mL) and extracted with CH₂Cl₂ (3 × 80 mL). The combined organic layers were dried (Na₂SO₄), the solvent was evaporated, and the remaining oily residue was coevaporated with toluene (3 × 10 mL) to afford a foamy residue which was applied to FC (silica gel, column 10 × 4 cm, CH₂Cl₂/MeOH, 95:5 → 90:10). Evaporation of the main zone afforded 11 as colorless foam (855 mg, 83%): TLC (CH₂Cl₂/MeOH, 90:10) *R*_f 0.53; λ_{max} (MeOH)/nm 236 (ε/dm³ mol⁻¹ cm⁻¹ 33700), 246 (29400), 300 (25900); ¹H NMR (DMSO-*d*₆, 300 MHz) (δ, ppm) 2.19–2.28 (m, 1H, 2'-H_α), 2.65–2.72 (m, 1H, 2'-H_β), 3.06 (s, 3H, NCH₃), 3.19 (s, 3H, NCH₃), 3.36 (m, 2H, 5'-H₂), 3.71 (s, 6H, 2 × OCH₃), 3.87–3.89 (m, 1H, 4'-H), 4.41 (s, 1H, C≡CH), 4.47–4.51 (m, 1H, 3'-H), 5.32–5.34 (d, *J* = 4.8 Hz, 1H, 3'-OH), 6.48 (t, *J* = 4.2 Hz, 1H, 1'-H), 6.77–6.82 (m, 4H, H-phenyl), 7.16–7.34 (m, 9H, H-phenyl), 8.71 (s, 1H, N=CH), 11.43 (s, 1H, HN). Anal. Calcd for C₃₆H₃₆N₆O₆ (648.27): C, 66.65; H, 5.59; N, 12.96. Found: C, 66.58; H, 5.66; N, 12.83.

6-[[[(Dimethylamino)methylidene]amino]-1-[2-deoxy-5-O-(4,4'-dimethoxytriphenylmethyl)-β-D-erythro-pentofuranosyl]-1,5-dihydro-3-ethynyl-4H-pyrazolo[3,4-d]pyrimidin-4-one 3'-[(2-Cyanoethyl)-*N,N*-(diisopropyl)]phosphoramidite (12). A solution of 11 (560 mg, 0.86 mmol) in anhydrous CH₂Cl₂ (10 mL) was treated with anhydrous (iPr)₂NEt (300 μL, 1.34 mmol) at rt. Then 2-cyanoethyl diisopropylphosphoramidochloridite (320 μL, 1.77 mmol) was added. After 3 h, the solution was washed with saturated NaHCO₃ and extracted with CH₂Cl₂ (2 × 100 mL). The combined organic layer was dried (Na₂SO₄), and the solvent was evaporated. FC (silica gel, column 8 × 3 cm, CH₂Cl₂/MeOH, 95:5) afforded 12 as a colorless foam (540 mg, 74%): TLC (CH₂Cl₂/MeOH, 95:5) *R*_f 0.74; ³¹P NMR (CDCl₃, 121.5 MHz) (δ, ppm) 148.36. Anal. Calcd for C₄₅H₅₃N₈O₇P (848.38): C, 63.67; H, 6.29; N, 13.20. Found: C, 63.89; H, 6.36; N, 13.20.

Monofunctionalization of 1,4-Bis-azidomethylbenzene (3) with Nucleosides 1 and 2. **6-Amino-1-(2-deoxy-β-D-erythro-pentofuranosyl)-1,5-dihydro-3-[1-(4-azidomethylbenzyl)-1H-[1,2,3-triazol-4-yl]]-4H-pyrazolo[3,4-d]pyrimidin-4-one (4).** To a solution of compound 1 (58.3 mg, 0.2 mmol) and 3 (188 mg, 1.0 mmol) in THF–H₂O–*t*-BuOH, 3:1:1 (3 mL) was added a freshly prepared 1 M solution of sodium ascorbate (159 μL, 0.16 mmol) in water, followed by the addition of copper(II) sulfate pentahydrate 7.5% in water (128 μL, 0.038 mmol). The reaction mixture was stirred in the dark at room temperature for 12 h. After completion of the reaction (monitored by TLC), the solvent was evaporated, and the residue was applied to FC (silica gel, column 8 × 3 cm, eluted with CH₂Cl₂/MeOH, 95:5 → 90:10). Evaporation of the main zone gave 4 as a pale yellow solid (71 mg, 74%): TLC (CH₂Cl₂/MeOH, 80:20) *R*_f 0.60; λ_{max} (MeOH)/nm 246 (ε/dm³ mol⁻¹ cm⁻¹ 48600), 260 (26000), 280 (12000). ¹H NMR (DMSO-*d*₆, 300 MHz) (δ, ppm) 2.15–2.23 (m, 1H, 2'-H_α), 2.74–2.83 (m, 1H, 2'-H_β), 3.40–3.44 (m, 1H, 5'-H), 3.51–3.56 (m, 1H, 5'-H), 3.77–3.80 (m, 1H, 4'-H), 4.44–4.49 (m, 3H, 3'-H, PhCH₂), 4.79 (t, *J* = 5.7 Hz, 1H, 5'-OH), 5.26–5.27 (d, *J* = 4.2 Hz, 1H, 3'-OH), 5.75 (s, 2H, PhCH₂), 6.36 (t, *J* = 6.3 Hz, 1H, 1'-H),

6.78 (br s, 2H, NH₂), 7.32–7.41 (m, 4H, H-phenylene), 8.95 (s, 1H, H-triazole), 10.75 (s, 1H, HN); ESI-TOF calcd for C₂₀H₂₁N₁₁O₄Na (M + Na⁺) 502.1670, *m/z* found 502.1671. Anal. Calcd for C₂₀H₂₁N₁₁O₄ (479.45): C, 50.10; H, 4.41; N, 32.14. Found: C, 50.10; H, 4.51; N, 31.95.

6-Amino-1-(2-deoxy-β-D-erythro-pentofuranosyl)-1,5-dihydro-3-[[1-(4-azidomethylbenzyl)-1H-(1,2,3-triazol-4-yl)]hexylidene]-4H-pyrazolo[3,4-d]pyrimidin-4-one (5). To a solution of compound 2 (74.2 mg, 0.2 mmol) and 3 (188 mg, 1.0 mmol) in THF–H₂O–*t*-BuOH, 3:1:1 (3 mL) was added a freshly prepared 1 M solution of sodium ascorbate (159 μL, 0.16 mmol) in water, followed by the addition of copper(II) sulfate pentahydrate 7.5% in water (128 μL, 0.038 mmol). The reaction mixture was stirred in the dark at room temperature for 12 h. After completion of the reaction (monitored by TLC), the solvent was evaporated, and the residue was applied to FC (silica gel, column 8 × 3 cm, eluted with CH₂Cl₂/MeOH, 95:5 → 90:10 → 80:20). The main zone afforded 5 as a colorless solid (67 mg, 60%): TLC (CH₂Cl₂/MeOH, 90:10) *R*_f 0.58; λ_{max} (MeOH)/nm 243 (ε/dm³ mol⁻¹ cm⁻¹ 51200), 280 (sh) (13100); ¹H NMR (DMSO-*d*₆, 300 MHz) (δ, ppm) 1.55–1.60 (m, 2H, CH₂), 1.73–1.77 (m, 2H, CH₂), 2.12–2.15 (m, 1H, 2'-H_α), 2.45–2.50 (m, 3H, CH₂, 2'-H_β), 2.64–2.68 (m, 4H, 2x CH₂), 3.43–3.49 (m, 1H, 5'-H), 3.75–3.76 (m, 1H, 4'-H), 4.35 (s, 1H, 3'-H), 4.42 (s, 2H, PhCH₂), 4.73 (m, 1H, 5'-OH), 5.23 (s, 1H, 3'-OH), 5.55 (s, 2H, PhCH₂), 6.27 (t, *J* = 6.3 Hz, 1H, 1'-H), 6.73 (br s, 2H, NH₂), 7.29–7.37 (m, 4H, H-phenylene), 7.94 (s, 1H, H-triazole), 10.68 (s, 1H, HN); ESI-TOF calcd for C₂₆H₂₉N₁₁O₄Na (M + Na⁺) 582.2296, *m/z* found 582.2300. Anal. Calcd for C₂₆H₂₉N₁₁O₄ (559.58): C, 55.81; H, 5.22; N, 27.53. Found: C, 56.17; H, 5.24.

Bis[6-Amino-1-(2-deoxy-β-D-erythro-pentofuranosyl)-1,5-dihydro-3-[[1-methylbenzyl-1H-(1,2,3-triazol-4-yl)]hexylidene]-4H-pyrazolo[3,4-d]pyrimidin-4-one] (7). Evaporation of the minor zone gave 7 as a white powder (14 mg, 15%). Analytical data are identical with already published data.²³

“Bis-click” Cross-Linking of Nucleoside 1 with 1,4-Bis-azidomethylbenzene (3). **Bis[6-Amino-1-(2-deoxy-β-D-erythro-pentofuranosyl)-1,5-dihydro-3-[1-methylbenzyl-1H-(1,2,3-triazol-4-yl)]-4H-pyrazolo[3,4-d]pyrimidin-4-one] (6).** To a solution of compound 1 (116.6 mg, 0.4 mmol) and 3 (37.6 mg, 0.2 mmol) in THF–H₂O–*t*-BuOH, 3:1:1 (6 mL) was added a freshly prepared 1 M solution of sodium ascorbate (318 μL, 0.32 mmol) in water, followed by the addition of copper(II) sulfate pentahydrate 7.5% in water (256 μL, 0.076 mmol), and the reaction mixture was stirred at room temperature for 12 h. After completion of the reaction (monitored by TLC), the mixture was filtered and the solid residue was washed with methanol (5 mL) and water (5 mL). Compound 6 was obtained as a yellow solid (80 mg, 52%): λ_{max} (0.1 M NaOH)/nm 242 (ε/dm³ mol⁻¹ cm⁻¹ 47 500), 260 (sh) (31800); ¹H NMR (DMSO-*d*₆, 300 MHz) (δ, ppm) 2.11–2.18 (m, 2H, 2'-H_α), 2.76–2.80 (m, 2H, 2'-H_β), 3.51–3.55 (m, 4H, 5'-H₂), 3.78–3.79 (m, 2H, 4'-H), 4.43–4.47 (m, 2H, 3'-H), 4.78 (t, *J* = 5.1 Hz, 2H, 5'-OH), 5.25–5.26 (d, *J* = 3.3 Hz, 2H, 3'-OH), 5.72 (s, 4H, 2 × PhCH₂), 6.35 (t, *J* = 6.0 Hz, 2H, 1'-H), 6.76 (br s, 4H, 2 × H₂N), 7.33–7.40 (m, 4H, H-phenylene), 8.94 (s, 2H, 2 × H-triazole), 10.74 (s, 2H, 2 × HN). Anal. Calcd for C₃₂H₃₄N₁₆O₈ (770.71): C, 49.87; H, 4.45; N, 29.08. Found: C, 49.49; H, 4.22; N, 28.65.

6-Amino-1-(2-deoxy-β-D-erythro-pentofuranosyl)-1,5-dihydro-3-[1-(4-azidomethylbenzyl)-1H-[1,2,3-triazol-4-yl]]-4H-pyrazolo[3,4-d]pyrimidin-4-one (4). The remaining solution was evaporated to dryness, and the residue was applied to FC (silica gel, column 8 × 3 cm, eluted with CH₂Cl₂/MeOH, 95:5 → 90:10). Compound 4 was isolated as a white powder (14 mg, 7%). For analytical data of 4, see above.

General Procedure for the “Stepwise Click” Huisgen–Sharpless–Meldal [3 + 2] Cycloaddition. Azidomethylbenzyl-Labeled Oligonucleotides (ODN-22–ODN-27) Using Oligonucleotides ODN-16–ODN-21 and the Bis-Azide 3 (“1.Click”). To the single-stranded oligonucleotide (5 A₂₆₀ units) were

added a mixture of the CuSO₄–TBTA ligand complex (50 μL of a 20 mM stock solution in H₂O/DMSO/*t*-BuOH, 4:3:1 for TBTA; 50 μL of a 20 mM stock solution in H₂O/DMSO/*t*-BuOH, 4:3:1 for CuSO₄), tris(carboxyethyl)phosphine (TCEP; 50 μL of a 20 mM stock solution in water), 1,4-bis-azidomethylbenzene **3** (37.5 μL of a 20 mM stock solution in dioxane/H₂O, 1:1), sodium bicarbonate (50 μL of a 20 mM aq solution), and 30 μL of DMSO, and the reaction proceeded at room temperature for 12 h. The reaction mixture was concentrated in a SpeedVac and dissolved in 1 mL of bidistilled water and centrifuged for 20 min at 12000 rpm. The supernatant solution was collected and further purified by reversed-phase HPLC (gradient III) to give about 60–80% isolated yield of the azidomethylbenzyl oligonucleotides ODN-22–ODN-27. The molecular masses of the azidomethylbenzyl oligonucleotides ODN-22–ODN-27 were determined by MALDI-TOF or LC-ESI-TOF mass spectrometry (Table S3, Supporting Information).

Cross-Linked Oligonucleotides (ICL-28step–ICL-33step) Using Azidomethylbenzyl Oligonucleotides ODN-22–ODN-27 and Alkynylated Oligonucleotides ODN-16, ODN-17, ODN-19 or ODN-20 (“2.click”). To the alkynylated oligonucleotide (ODN-16, ODN-17, ODN-19, or ODN-20; 2 A₂₆₀ units) and azidomethylbenzyl oligonucleotide (ODN-22–ODN-27; 1.5 A₂₆₀ units) were added a mixture of the CuSO₄–TBTA ligand complex (10 μL of a 20 mM stock solution in H₂O/DMSO/*t*-BuOH, 4:3:1 for TBTA; 10 μL of a 20 mM stock solution in H₂O/DMSO/*t*-BuOH, 4:3:1 for CuSO₄), tris(carboxyethyl)phosphine (TCEP; 10 μL of a 20 mM stock solution in water), sodium bicarbonate (5 μL of a 200 mM aq. solution), and 7 μL of DMSO, and the reaction proceeded at room temperature for 12 h. The reaction mixture was concentrated in a SpeedVac and dissolved in 1 mL of bidistilled water and centrifuged for 20 min at 12000 rpm. The supernatant solution was collected and further purified by reversed-phase HPLC (gradient III) to give about 40–50% isolated yield of the cross-linked oligonucleotides ICL-28step–ICL-33step. The molecular masses of the cross-linked oligonucleotides ICL-28step–ICL-33step were determined by MALDI-TOF or ESI-TOF mass spectrometry (Table S3, Supporting Information).

■ ASSOCIATED CONTENT

S Supporting Information. Mass spectra of non-cross-linked and cross-linked oligonucleotides, coupling constants of the stepwise and bis-click derivatives, HPLC purification profiles of azidomethylbenzyl-labeled oligonucleotides and cross-linked oligonucleotides, melting curves of ICLs, ¹H NMR, ¹³C NMR, DEPT-135 and ¹H–¹³C-gated decoupled NMR spectra of the new compounds **1**, **4–6**, and **9–12** and ³¹P NMR spectra of phosphoramidite **12**. This material is available free of charge via the Internet at <http://pubs.acs.org>.

■ AUTHOR INFORMATION

Corresponding Author

*Tel: +49 (0)251-53406-500. Fax: +49 (0)251-53406-587. E-mail: frank.seela@uni-osnabrueck.de. Web: www.seela.net.

■ ACKNOWLEDGMENT

We thank Dr. S. Budow for her continuous support throughout the preparation of the manuscript. We thank S. S. Pujari for measuring the NMR spectra and appreciate critical reading of the manuscript by Dr. P. Leonard, N. Q. Tran for oligonucleotide synthesis, Dr. Uhlmann, Coley Pharmaceuticals GmbH for ESI mass spectra, and Dr. R. Thiele from Roche Diagnostics, Penzberg,

for the measurement of the MALDI spectra. Financial support by ChemBiotech, Muenster, Germany, is gratefully acknowledged.

■ REFERENCES

- (1) Noll, D. M.; McGregor Mason, T.; Miller, P. S. *Chem. Rev.* **2006**, *106*, 277–301.
- (2) Alzeer, J.; Schärer, O. D. *Nucleic Acids Res.* **2006**, *34*, 4458–4466.
- (3) Xu, X.; Muller, J. G.; Ye, Y.; Burrows, C. J. *J. Am. Chem. Soc.* **2008**, *130*, 703–709.
- (4) Rajski, S. R.; Williams, R. M. *Chem. Rev.* **1998**, *98*, 2723–2795.
- (5) Cadet, J.; Vigny, R. In *Bioorganic Photochemistry*; Morrison, H., Ed.; Wiley: New York, 1990; pp 1–272.
- (6) Ding, H.; Greenberg, M. M. *J. Org. Chem.* **2010**, *75*, 535–544.
- (7) Rink, S. M.; Lipman, R.; Alley, S. C.; Hopkins, P. B.; Tomasz, M. *Chem. Res. Toxicol.* **1996**, *9*, 382–389.
- (8) Cimino, G. D.; Gamper, H. B.; Isaacs, S. T.; Hearst, J. E. *Annu. Rev. Biochem.* **1985**, *54*, 1151–1193.
- (9) (a) Huisgen, R.; Szeimies, G.; Möbius, L. *Chem. Ber.* **1967**, *100*, 2494–2507. (b) Huisgen, R. *Pure Appl. Chem.* **1989**, *61*, 613–628.
- (10) (a) Tornøe, C. W.; Christensen, C.; Meldal, M. *J. Org. Chem.* **2002**, *67*, 3057–3064. (b) Meldal, M.; Tornøe, C. W. *Chem. Rev.* **2008**, *108*, 2952–3015.
- (11) Rostovtsev, V. V.; Green, L. G.; Fokin, V. V.; Sharpless, K. B. *Angew. Chem., Int. Ed.* **2002**, *41*, 2596–2599.
- (12) (a) Gramlich, P. M. E.; Wirges, C. T.; Manetto, A.; Carell, T. *Angew. Chem., Int. Ed.* **2008**, *47*, 8350–8358. (b) El-Sagheer, A. H.; Brown, T. *Chem. Soc. Rev.* **2010**, *39*, 1388–1405.
- (13) (a) Tron, G. C.; Pirali, T.; Billington, R. A.; Canonico, P. L.; Sorba, G.; Genazzani, A. A. *Med. Res. Rev.* **2008**, *28*, 278–308. (b) Jawalekar, A. M.; Meeuwenoord, N.; Cremers, J. G. O.; Overkleeft, H. S.; van der Marel, G. A.; Rutjes, F. P. J. T.; van Delft, F. L. J. *Org. Chem.* **2008**, *73*, 287–290. (c) Pourceau, G.; Meyer, A.; Vasseur, J.-J.; Morvan, F. J. *Org. Chem.* **2009**, *74*, 1218–1222.
- (14) Kiviniemi, A.; Virta, P.; Lönnberg, H. *Bioconjugate Chem.* **2008**, *19*, 1726–1734.
- (15) El-Sagheer, A. H.; Brown, T. *J. Am. Chem. Soc.* **2009**, *131*, 3958–3964.
- (16) Alvira, M.; Eritja, R. *Chem. Biodiv.* **2007**, *4*, 2798–2809.
- (17) Nakane, M.; Ichikawa, S.; Matsuda, A. *J. Org. Chem.* **2008**, *73*, 1842–1851.
- (18) Amblard, F.; Cho, J. H.; Schinazi, R. F. *Chem. Rev.* **2009**, *109*, 4207–4220.
- (19) Peng, X.; Li, H.; Seidman, M. *Eur. J. Org. Chem.* **2010**, 4194–4197.
- (20) (a) Kumar, R.; El-Sagheer, A.; Tumpene, J.; Lincoln, P.; Wilhelmsson, L. M.; Brown, T. *J. Am. Chem. Soc.* **2007**, *129*, 6859–6864. (b) El-Sagheer, A. H.; Kumar, R.; Findlow, S.; Werner, J. M.; Lane, A. N.; Brown, T. *ChemBioChem* **2008**, *9*, 50–52. (c) Kočalka, P.; El-Sagheer, A. H.; Brown, T. *ChemBioChem* **2008**, *9*, 1280–1285.
- (21) Jacobsen, M. F.; Ravnsbæk, J. B.; Gothelf, K. V. *Org. Biomol. Chem.* **2010**, *8*, 50–52.
- (22) Holub, J. M.; Kirshenbaum, K. *Chem. Soc. Rev.* **2010**, *39*, 1325–1337.
- (23) Pujari, S. S.; Xiong, H.; Seela, F. *J. Org. Chem.* **2010**, *75*, 8693–8696.
- (24) Best, M. D. *Biochemistry* **2009**, *48*, 6571–6584.
- (25) (a) Prescher, J. A.; Bertozzi, C. R. *Nature Chem. Biol.* **2005**, *1*, 13–21. (b) Baskin, J. M.; Bertozzi, C. R. *QSAR Comb. Sci.* **2007**, *26*, 1211–1219. (c) Jewett, J. C.; Bertozzi, C. R. *Chem. Soc. Rev.* **2010**, *39*, 1272–1279.
- (26) van Swieten, P. F.; Leeuwenburgh, M. A.; Kessler, B. M.; Overkleeft, H. S. *Org. Biomol. Chem.* **2005**, *3*, 20–27.
- (27) (a) Seela, F.; Sirivolu, V. R. *Chem. Biodiv.* **2006**, *3*, 509–514. (b) Seela, F.; Sirivolu, V. R.; Chittepudi, P. *Bioconjugate Chem.* **2008**, *19*, 211–224. (c) Seela, F.; Xiong, H.; Leonard, P.; Budow, S. *Org. Biomol. Chem.* **2009**, *7*, 1374–1387. (d) Qing, G.; Xiong, H.; Seela, F.; Sun, T. *J. Am. Chem. Soc.* **2010**, *132*, 15228–15232. (e) Seela, F.; Ingale,

- S. A. *J. Org. Chem.* **2010**, *75*, 284–295. (f) Seela, F.; Pujari, S. S. *Bioconjugate Chem.* **2010**, *21*, 1629–1641.
- (28) Bräse, S.; Banert, K. *Organic Azides*; John Wiley & Sons: Chichester, 2010.
- (29) Scriven, E. F. V.; Turnbull, K. *Chem. Rev.* **1988**, *88*, 297–368.
- (30) Thomas, J. R.; Liu, X.; Hergenrother, P. J. *J. Am. Chem. Soc.* **2005**, *127*, 12434–12435.
- (31) (a) Seela, F.; He, Y.; He, J.; Becher, G.; Kröschel, R.; Zulauf, M.; Leonard, P. In *Methods in Molecular Biology*; Herdewijn, P., Ed.; Humana Press: Totowa, NJ, 2004; Vol. 288, pp 165–86. (b) Seela, F.; Becher, G. *Synthesis* **1998**, 207–214. (c) Seela, F.; Becher, G. *Chem. Commun.* **1998**, 2017–2018.
- (32) (a) Seo, T. S.; Li, Z.; Ruparel, H.; Ju, J. *J. Org. Chem.* **2003**, *68*, 609–612. (b) Seo, T. S.; Bai, X.; Ruparel, H.; Li, Z.; Turro, N. J.; Ju, J. *Proc. Natl. Acad. Sci. U.S.A.* **2004**, *101*, 5488–5493.
- (33) Miller, G. P.; Kool, E. T. *J. Org. Chem.* **2004**, *69*, 2404–2410.
- (34) (a) Lietard, J.; Meyer, A.; Vasseur, J.-J.; Morvan, F. *Tetrahedron Lett.* **2007**, *48*, 8795–8798. (b) Lietard, J.; Meyer, A.; Vasseur, J.-J.; Morvan, F. *J. Org. Chem.* **2008**, *73*, 191–200.
- (35) Jiang, D.; Seela, F. *J. Am. Chem. Soc.* **2010**, *132*, 4016–4024.
- (36) (a) Endo, M.; Majima, T. *Angew. Chem., Int. Ed.* **2003**, *42*, 5744–5747. (b) Endo, M.; Majima, T. *J. Am. Chem. Soc.* **2003**, *125*, 13654–13655.
- (37) Wilds, C. J.; Noronha, A. M.; Robidoux, S.; Miller, P. S. *J. Am. Chem. Soc.* **2004**, *126*, 9257–9265.
- (38) (a) Angelov, T.; Guainazzi, A.; Schärer, O. D. *Org. Lett.* **2009**, *11*, 661–664. (b) Guainazzi, A.; Campbell, A. J.; Angelov, T.; Simmerling, C.; Schärer, O. D. *Chem.—Eur. J.* **2010**, *16*, 12100–12103.
- (39) (a) Hong, I. S.; Greenberg, M. M. *J. Am. Chem. Soc.* **2005**, *127*, 3692–3693. (b) Peng, X.; Greenberg, M. M. *Nucleic Acids Res.* **2008**, *36*, e31.
- (40) (a) Stevens, K.; Madder, A. *Nucleic Acids Res.* **2009**, *37*, 1555–1565. (b) Bellon, S.; Gasparutto, D.; Saint-Pierre, C.; Cadet, J. *Org. Biomol. Chem.* **2006**, *4*, 3831–3837.
- (41) (a) Kolb, H. C.; Finn, M. G.; Sharpless, K. B. *Angew. Chem., Int. Ed.* **2001**, *40*, 2004–2021. (b) Kolb, H. C.; Sharpless, K. B. *Drug Disc. Today* **2003**, *8*, 1128–1137.
- (42) Helms, B.; Mynar, J. L.; Hawker, C. J.; Fréchet, J. M. J. *J. Am. Chem. Soc.* **2004**, *126*, 15020–15021.
- (43) Chow, H.-F.; Lau, K.-N.; Ke, Z.; Liang, Y.; Lo, C.-M. *Chem. Commun.* **2010**, 46, 3437–3453.
- (44) Binder, W. H.; Sachsenhofer, R. *Macromol. Rapid Commun.* **2007**, *28*, 15–54.
- (45) Johnson, J. A.; Finn, M. G.; Koberstein, J. T.; Turro, N. J. *Macromol. Rapid Commun.* **2008**, *29*, 1052–1072.
- (46) (a) Moses, J. E.; Moorhouse, A. D. *Chem. Soc. Rev.* **2007**, *36*, 1249–1262. (b) Hein, J. E.; Fokin, V. V. *Chem. Soc. Rev.* **2010**, *39*, 1302–1315.
- (47) Díaz, D. D.; Punna, S.; Holzer, P.; McPherson, A. K.; Sharpless, K. B.; Fokin, V. V.; Finn, M. G. *J. Polym. Sci., Part A: Polym. Chem.* **2004**, *42*, 4392–4403.
- (48) *User's Manual of the DNA Synthesizer*; Applied Biosystems, Weiterstadt, Germany.
- (49) Petersheim, M.; Turner, D. H. *Biochemistry* **1983**, *22*, 256–263.
- (50) Seela, F.; Wenzel, T. *Helv. Chim. Acta* **1992**, *75*, 1111–1122.